HHS Public Access

Author manuscript

Dev Biol. Author manuscript; available in PMC 2017 July 01.

Published in final edited form as:

Dev Biol. 2016 July 1; 415(1): 98–110. doi:10.1016/j.ydbio.2016.04.013.

Pias1 is essential for erythroid and vascular development in the mouse embryo

Jerfiz D. Constanzo[1], **Mi Deng**[2], **Smita Rindhe**[1], **Ke-jing Tang**[1,3], **Cheng-cheng Zhang**[2], and **Pier Paolo Scaglioni**[1,*]

[1]Department of Internal Medicine and Simmons Cancer Center, University of Texas Southwestern Medical Center Dallas, TX 75390, USA

[2]Departments of Physiology, and Developmental Biology, University of Texas Southwestern Medical Center Dallas, TX 75390, USA

[3]Department of Pulmonary Medicine, The First Affiliated Hospital of Sun Yat-sen University, Guangzhou, Guangdong 510080, China

Abstract

The protein inhibitor of activated STAT-1 (PIAS1) is one of the few known SUMO E3 ligases. PIAS1 has been implicated in several biological processes including repression of innate immunity and DNA repair. However, PIAS1 function during development and tissue E12.5. We found significant apoptosis within the yolk sac (YS) blood vessels and concomitant loss of red blood cells (RBCs) resulting in profound anemia. In addition, *Pias1* loss impairs YS angiogenesis and results in defective capillary plexus formation and blood vessel occlusions. Moreover, heart development is impaired as a result of loss of myocardium muscle mass. Accordingly, we found that *Pias1* expression in primary myoblasts enhances the induction of cardiac muscle genes *MyoD, Myogenin* and *Myomaker*. PIAS1 protein regulation of cardiac gene transcription is dependent on transcription factors *Myocardin* and *Gata-4*. Finally, endothelial cell specific inactivation of *Pias1 in vivo* impairs YS erythrogenesis, angiogenesis and recapitulates loss of myocardium muscle mass. However, these defects are not sufficient to recapitulate the lethal phenotype of *Pias1* null embryos. These findings highlight *Pias1* as an essential gene for YS erythropoiesis and vasculogenesis *in vivo*.

Keywords

Pias1; fetal erythropoiesis; angiogenesis; yolk sac capillary plexus; embryonic development

[*]**Corresponding author:** Dr. Pier Paolo Scaglioni, MD, 5323 Harry Hines Boulevard, TX 5323-8852, Tel: +1214 645 6449, Fax: +12146455915. Pier.Scaglioni@UTSouthwestern.edu.

Author Contributions

J.D.C. and P.P.S. conceived the project; J.D.C., M.D, S.R. and K.T. Performed experiments; J.D.C and PPS wrote the manuscript.

Introduction

The cardiovascular system is critical during embryonic development. The vasculature supplies the developing embryo with oxygen, nutrients and removes metabolic waste. Consequently, inactivation of genes that impair vascular or erythroid development result in mouse embryonic lethality (Shalaby et al., 1995; Conway et al., 2003; Maeda et al., 2009; Pang et al., 2012). The first nucleated RBCs, also called primitive erythrocytes, are visible within the yolk sac (YS) blood islands approximately at embryonic (E) days 7.5-8.5. These nucleated red blood cells begin circulating the embryo proper at E8.5 after the YS and dorsal aorta (DA) blood vessels have fused (Conway et al., 2003). Vasculogenesis, de-novo generation of blood vessels, starts following new blood cells formation, between E7.5 and E8.5 (Coffin et al., 1991; Coffin and Poole, 1991). The vascular and erythroid cell compartments cooperate to promote embryonic growth via nutrient delivery and gaseous exchange.

Endothelial cells are essential for the onset of erythropoiesis in the mouse embryo. For instance, they give rise to the primitive erythroid cell lineage in the YS and blood vessels from a common progenitor called the hemangioblast (Auerbach et al., 1996; Lacaud et al., 2001). These cells then colonize the fetal liver and therein maintain hematopoiesis until birth. In addition, a direct interaction between hematopoietic stem and progenitor cells (HSPCs) and the vascular endothelium has been reported during asymmetric cell divisions in zebrafish (Jacobsen et al., 2014; Tamplin et al., 2015). To achieve this complex multicellular task, key transcription factors, cytokines, growth factors and their plasma membrane receptors are required to orchestrate proper erythroid and vascular development. For instance, transcription factors GATA-1, GATA-4 and MYC are required for proper cardiovascular and RBC development in mice.

Disruption of either *Gata1* or *Myc* alters the gene expression profiles of hematopoietic stem cells, resulting in anemia, endothelial cell apoptosis and embryonic lethality (Baudino et al., 2002; Yu et al., 2010; Pang et al., 2012), while disruption of *Gata-4* results in cardiovascular failure and abnormal heart development (Kelley et al., 1993; Ip et al., 1994). Plasma membrane receptors controlled by *Gata1* or *Myc*, such as vascular endothelial growth factor receptors 1/2 (VEGFR1/2) and their ligand VEGF enhance pro-survival signaling and define the formation and directionality of new blood vessels and the lymphatic systems (Shalaby et al., 1995; Stefater et al., 2011; Dellinger et al., 2013). Moreover, vascular cell adhesion molecule-1 (*Vcam-1*) gene expression in endothelial cells regulates the interaction between the vascular endothelium and RBCs, promoting RBCs survival and differentiation (Sturgeon et al., 2012; Jacobsen et al., 2014).

On the other hand, three key regulatory proteins Semaphorin-3A/E (SEMA3A; SEMA3E), Thrombspondin-1 (THBS1) and bone morphogenesis protein 2 (BMP2), provide the restrictive signals that block blood and lymphatic vessel formation in the mouse. SEMA3A/E protein, for instance, promotes retraction of cell projections and inhibits endothelial cell adhesion to extracellular matrix, while THBS1 and BMP2 proteins are anti-angiogenic by inhibiting migration and proliferation of endothelial cells (Meadows et al., 2013; Dunworth et al., 2014; McKenna et al., 2014; Feng et al., 2015).

An emerging layer of complexity in these developmental processes is the contribution of posttranslational modifications on transcription factors and heterochromatin remodeling. Modifications with small ubiquitin-like modifiers (SUMO) have recently gained attention because of their participation in activation/repression of gene transcription (Yu et al., 2010; Costa et al., 2011; Liu et al., 2014b). SUMOylation of target proteins alters their function by promoting changes in protein-protein interaction and/or heterochromatin accessibility.

SUMOylation is a multistep process in which SUMO proteins are added onto substrates by the stepwise transfer of SUMO from activating enzyme E1, cargo enzyme E2 and finally onto conjugating enzyme E3 ligase (Palvimo, 2007; Rytinki et al., 2009). For instance the E2 ligase UBC9 is required during chromosome segregation and genomic stability in mice and for maintaining hematopoietic stem cell self-renewal in Drosophila melanogaster (Nacerddine et al., 2005; Kalamarz et al., 2012). Moreover, PIAS-like protein ZIMP10 was shown to contribute to vascular and hematopoietic development in mice (Beliakoff et al., 2008).

PIAS1 loss was reported to result in embryonic and perinatal lethality in mice, but a detailed examination of these events has not been performed (Beliakoff et al., 2008). The goal of our study was to provide a better understanding of the role of PIAS1 in the regulation biological processes in multicellular organisms during embryonic development. To do this, we generated two novel mouse mutant strains that constitutively or conditionally inactivate the Pias1 gene. We analyzed embryos at different stages of development and characterized the individual tissues affected for defects in cell proliferation and differentiation.

Materials And Methods

Mouse ES Cells and Mouse genotyping

Embryonic stem cells (ESC) for *Pias1* gene constitutive inactivation were generated by the UC DAVIS Mutant Mouse Resource and Research Centers (MMRRC; www.mmrrc.org), clone $Pias1^{RRQ113}$. Genotyping primers used for real times (RT-PCR) were as follows: FW. ATGGCGGACAGTGCGGAACTAA; RV1.CTGTTGTGGTGTCAAGGCAAAT; RV2. GACATATCGGCCTCAGGAAG. ES cells for *Pias1* gene conditional inactivation were generated by the NIH Knock-Out Mouse Project (KOMP) and obtained from the KOMP Repository (www.komp.org), clone $Pias1^{tm1a(KOMP)Wtsi}$. Genotyping primers (floxed): FW1. GAGATGGCGCAACGCAATTAATG; RV1. ATGCCCTCAGAAGCAATGAAAGAGC; (wt) FW2. CAGCAGATCAGCAGCTCCAT; RV2. CAGATGCAGCTTCCGGACTA. All experimental procedures involving animals in this study were reviewed and approved by the University of Texas Southwestern Medical Center Institutional Animal Care and Use Committee (IACUC).

LacZ reporter assay and X-gal staining

For whole-mount X-gal staining, embryos were fixed in cold 4% PFA/1xPBS buffer (0.1% deoxycholic acid; 0.2% Igepal-NP40) for 45 min at 4°C with gentle shaking. Embryos were rinsed twice with cold 1xPBS, stained overnight using staining buffer (5 mM $K_3Fe(CN)_6$; 5

mM $K_4Fe(CN)_6$; 2 mM $MgCl_2$; 1 mg/ml X-gal in 1xPBS) followed by two 1xPBS washes and post-fixing with 4% PFA/PBS and glutaraldehyde (Millay et al., 2013).

Cryosection and immunofluorescence

Frozen sections of E7.5-E8.0 embryos were used. Tissues sections were permeabilized with 0.3% Triton X-100 in 1xPBS, blocked with 20% AquaBlock™ with 0.02% sodium azide for 1 hour, incubated with Ki67 1:500 (Cell signaling), PML 1: 500 (Santa Cruz, No.: sc-5621), C. CASPASE 3 1:500 (Cell signaling, No.: 9665) overnight. Primary antibodies were washed off tissue-slides twice with 1x PBS, slides were incubated in Alexa-Fluor secondary antibodies and 1:800 4', 6-diamidino-2-phenylindole (DAPI) for 30 mines. 40x magnification pictures were taken with a Leica DMI6000 inverted microscope. Picture analysis of fluorescence intensity was performed with ImageJ software.

Whole mount immunohistochemistry

Endogenous peroxydase was neutralized by incubating the embryos in 5% hydrogen peroxide for 5 hours RT. Background signal was reduced by incubating embryos in 20% AquaBlock™ (East Coast Biologics, cat no.: PP82-P0691), 0.1% TritonX-100 overnight. Finally, embryos were incubated with primary antibody against *Pecam* (CD31) in 5% AquaBlock™ 0.1% TritonX-100 overnight, washed 4 times in 0.1% Triton/1xPBS at 4°C with gentle agitation, incubated with HRP-conjugated secondary antibody, washed 3 times in 5% AquaBlock™/0.1% Triton/1xPBS for 30 minutes at RT, rinsed with 1xPBS for 20 min and stained using the DAB kit (Vector labs, No.: SK 4100).

Quantitative PCR (qPCR)

Total RNA was extracted from fresh/frozen tissues using the total RNA extraction kit from SIGMA (SIMA-Aldrich, No.: RTN350) following manufacturer's protocols. cDNA synthesis was done using Superscript III reverse transcriptase with random examer primers (Invitrogen, No: 18080-400). For qPCR analysis, we used Power SYBR Green (Applied Biosystems, No.: 4368577) detection-dye and followed manufacturer's protocol. To analyze the samples we used the *Applied Biosystems 7500 Fast Real-Time PCR System* (Applied Biosystems, No.: ABI-7500).

Methocult™ cell differentiation assays

Yolk sacs (YS) were isolated at 9.5. Approximately 1×10^3 cells diluted in 100 .L serum free media were mixed with 2 mL Methocult™ media (Stem cell tech. no.: 03436) supplemented with either recombinant mouse erythropoietin (rEPO) (R&D systems no.: 959-ME) or recombinant mouse granulocyte-macrophage colony stimulation factor (rGMCSF) (Millipore No.: GF206). Cells were allowed to form colonies for 5 days and then imaged in phase contrast using DMI6000 inverted microscope (Leica).

Cardiogenic differentiation

To induce cardiac differentiation following *Pias1* expression, primary myoblasts and mouse embryonic fibroblasts (MEFs) cell cultures were placed in differentiation media (2% horse serum, DMEM) for 3 days (Millay et al., 2013) followed by qPCR analysis.

Western blotting

Cells lysate was prepared with radioimmunoprecipitation assay buffer (RIPA buffer) with protease and phosphatase inhibitors. 40ug of proteins was resolved on 8% SDS-PAGE gel, transferred to nitrocellulose membrane and probed for the indicated antibodies.

Flow cytometry

Embryos from E9.5 to E12.5 were washed in cold 1xPBS, YS were processed to obtain single-cell suspensions using 1 mg/mL collagenase D (Roche)/ 3% FBS in PBS, gently rocking at 37C for 30 min. Finally single cells were washed 1X in PBS, resuspend in 3% FBS in DMEM, treated with fluorescently labeled CD71, Ter119, Mac1 and Gr1 antibodies and analyzed by FACS.

RNAi interference

Stable *PIAS1* knockdown was performed with pGIPZ vectors containing shRNA against *PIAS1* (5'-CCGGATCATTCTAGAGCTTTA-3' No.: TRCN0000231898); (5'-TTTGCTGGGCTTTGCTATTTC-3'; No.: TRCN0000231555) and non-targeting scrambled shRNA controls (Open biosystems, No.: RHS4346). Lentiviral particles were generated by transfection of HEK-293T cells with pGIPZ and helper plasmids (Addgene, No.: 84545; 8455). 4μg/mL Polybrene (SIGMA, No.: H9268) was used with viral supernatant to enhance transduction efficiency.

Results

Ablation of *Pias1* impairs embryonic development

We generated two strains of *Pias1* deficient mice using targeted ES cells. We used UC DAVIS $Pias1^{RRQ113}$ ES cell line to inactivate *Pias1* with a gene trap insertion after exon 1, introducing a polyadenylation site and a premature stop codon ($Pias1^{-/-}$ mice). We used KOMP Repository ES cell line $Pias1^{tm1a(KOMP)Wtsi}$ to generate mice that allow Cre recombinase-mediated excision of *LoxP* flanked exons 2 and 3 (*$Pias1^{f/f}$ mice*). *Pias1* gene was disrupted in both mouse lines as determined by real-time PCR (RT-PCR) and immunoblotting (Figure 1A-C and Suppl. Figure 1A-C). Next, we determined the pattern of *Pias1* gene expression in $Pias1^{+/-}$ embryos using the *LacZ* reporter inserted into the *Pias1* gene locus by the gene trap vector. Consequently, X-gal staining can be used as a proxy to assess *Pias1* gene expression. We found that X-gal staining first appeared in the embryo proper at E8.0-E8.25 and the staining became progressively stronger in the YS at E9.5 and E10.5 (Figure 1D).

Ablation of *Pias1* causes embryonic lethality with incomplete penetrance

Although $Pias1^{+/-}$ mice appear healthy and are fertile, their intercross leads to a 90% reduction in viable $Pias1^{-/-}$ progeny (Table 1A). To determine the timing of prenatal lethality, we analyzed embryos from timed pregnancies of $Pias1^{+/-}$ intercrosses. Between E12.5 and E15.5 the percentage of viable $Pias1^{-/-}$ embryos dropped to approximately 10% (Table 1B). Notably, the defects in the embryo and the YS temporally coincided with the induction of *Pias1* promoter activation, determined by X-Gal staining.

Ablation of Pias1 impairs YS erythropoiesis

We noticed that *Pias1*$^{-/-}$ null embryos develop without obvious morphological defects other than mild growth retardation until E9.5 (Suppl. Figure 2A and Suppl. Table 1). However, between E10.5 and E12.5 *Pias1*$^{-/-}$ embryos are significantly growth retarded, show a striking reduction in blood content in the YS and severe cardiomegaly (Figure 1E). Since the reduction in blood content in the YS is the first macroscopic defect that we detected, we analyzed the YS in more detail first and subsequently cardiovascular defects. We found that in *Pias1* heterozygous YS, the X-Gal stain is most prevalent in RBCs and endothelial cells lining the blood islands (Figure 1F). Strikingly, *Pias1* deficiency leads to loss RBCs content and aberrant capillary structures formation (Figure 1G-H). Notably, we found that GATA-1, a well-known erythroid transcription factor required for YS RBC differentiation and survival, and PIAS1 colocalize in RBCs present in blood islands; and that RBCs are depleted from *Pias1*$^{-/-}$ blood islands (Figure 1I). These findings indicate that *Pias1* is expressed and functionally relevant in erythroid precursors and endothelial cells forming the YS blood islands.

Taken together, these findings support the conclusion that loss of *Pias1* results in embryonic growth retardation and defective YS erythropoiesis, which becomes apparent after E10.5 and progressively becomes limiting causing embryonic lethality between E10.5 and 12.5 in 90% of embryos, with the majority of the embryos dying at day 12.5 (Table 1B).

PIAS1 regulates germ layer proliferation and survival during development

Aside from growth retardation, we observed no other obvious defects prior to E7.5-E8.5. Thus, we determined whether there was a defect in cellular proliferation or an increase in apoptosis that could explain the growth retardation phenotype. We stained by immunofluorescence (IF) cryosections of *Pias1*$^{+/+}$ and *Pias1*$^{-/-}$ embryos at E7.5-E8.0 (Figure 2A-C), using the proliferation marker Ki67, the apoptosis marker cleaved Caspase-3 (C.CASPASE-3) and the PIAS1 regulated tumor suppressor promyelocyteic leukemia (PML). Is important to note that PIAS1 has been reported to directly SUMOylate PML and to promote its ubiquitin-mediated degradation to promote cell survival (Rabellino et al., 2012).

We found that in *Pias1*$^{-/-}$ embryos, there is a significant decrease in Ki67 positivity/intensity in cells from the endoderm and mesoderm germ layers (Figure 2B; yellow arrows). In contrast, we observed an increase in Ki67 stain positivity in a group of cells from the ectoderm layer of *Pias1*$^{-/-}$ embryos as compared to *Pias1*$^{+/+}$controls (Figure 2B; red arrows). Moreover, *Pias1*$^{-/-}$ endoderm and mesoderm layer has a concomitant increase in PML and C.CASPASE-3 proteins positivity relative to *Pias1*$^{+/+}$ controls (Figure 2C; yellow arrows). Quantification of data obtained from the germ layers of independent embryos revealed that the percentage of Ki67 positive cells is consistently reduced in Pias1$^{-/-}$ embryos and that PML and C.CASPASE-3 are significantly increased (Figure 2D-E). PML has a well-known growth suppressive and pro-apoptotic function, which may explain the negative effects on embryonic germ layer development and embryonic growth retardation caused by *Pias1* loss (Bernardi and Pandolfi, 2003).

To determine whether the defect in germ layer proliferation is cell autonomous, we dissociated E8.5-E9.5 *Pias1*$^{+/+}$ and *Pias1*$^{-/-}$ embryos into single cells and used them to perform proliferation assays (Figure 2H). This analysis revealed that *Pias1* null embryonic cells were significantly fewer in number at the experimental end point, suggesting an intrinsic defect in their proliferative or survival capacity *in vitro*. Accordingly, we found a significant reduction in cell proliferation in *Pias1* conditional null mouse embryonic fibroblasts (MEFs) following acute *Pias1* gene inactivation using Adeno-Cre mediated recombination of *Pias1*$^{f/f}$ alleles (Figure 2I). Reduced cell proliferation coincided with an increase in PML and BIM-EL proapoptotic proteins and a decrease in cyclin D1, a marker of cell cycle progression, in *Pias1* conditional null MEFs (Figure 2J).

These findings suggest that *Pias1* inactivation negatively affects cell survival. Indeed, we determined that a significant percentage of *Pias1*$^{+/-}$ and *Pias1*$^{-/-}$ MEFs, when compared to *Pias1*$^{+/+}$ controls, accumulate Trypan blue (cell exclusion dye) 24h after plating *in vitro* (Suppl. Figure 2B). This result demonstrates increased membrane permeability and cell death. In vivo, we also observed PML and BIM upregulation in E12.5 liver tissue from *Pias1* deficient embryos, which at this stage is mostly comprised of erythroblast and their progeny (Suppl. Figure 2C).

In light of these findings, we concluded that *Pias1* loss result in uncoordinated proliferation of the germ layers at an early stage of embryonic development. This is evident by decreased proliferation of the endoderm/mesoderm layers and increased proliferation of the ectoderm layer. Furthermore, *Pias1* loss lowers the threshold for apoptosis in cells *in vivo* and *in vitro* and is particularly detrimental to hematopoietic-progenitor tissues.

Pias1 ablation impairs erythrocyte development while promoting macrophage differentiation

We determined whether RBC depletion in the YS was a result of an intrinsic defect in erythropoiesis or to a non-cell autonomous process such as loss of interaction with the endothelial niche. To do this, we characterized YSs at E9.5 when we start observing a defect in YS erythrocyte content. In the developing embryo, the vast majority of hematopoiesis is dedicated to the production of red blood cells. The paucity of other myeloid precursor cells, which amounts to less than 1% or erythroid precursor cells, renders their characterization by flow cytometry challenging at E.9.5. For this reason, we dissociated E9.5 YSs into single cell suspensions and induced erythroid differentiation *in vitro* with Methocult™ hematopoietic differentiation media. We used recombinant erythropoietin (rEPO) or recombinant granulocyte macrophage colony stimulating factor (rGMCSF) for 5 days to induce erythroid or myeloid differentiation (Sturgeon et al., 2012; Sturgeon et al., 2014). We discovered that hematopoietic precursors in *Pias1*$^{-/-}$ embryos were able to proliferate in Methocult™ media, but were deficient at forming mature erythroid cells *in vitro,* determined by heme accumulation (Figure 3A, red arrows). We also found that stimulation with rGMCSF leads to a significant enrichment of the macrophage cell lineage (Figure 3B, arrows).

To further characterize this phenotype, we compared endogenous hematopoietic cell populations present in the YS at E12.5 using flow cytometry. We used the transferin receptor

(CD71) as a marker for erythroid precursors and Ter119 for terminally differentiated erythroid cells. This analysis identifies several cell populations based on their differentiation stage: $CD71^{+}Ter119^{-}$ (R1) pro-erythroblast, $CD71^{+}Ter119^{+}$ (R2) early polychromatophilic erythroblast and $CD71^{-}Ter119^{+}$ (R3) poly/orthochromatophilic erythroblast and enucleated erythroblast (Maeda et al., 2009; Yu et al., 2010). We found a significant increase in the R1 population and a decrease in R2 and R3 cell population in the YS of *Pias1*$^{-/-}$ embryos (Figure 3C). This finding indicates that the severe embryonic anemia observed in *Pias1* null embryos is not due to lack of erythroid progenitors, but to impaired erythroid maturation consistent with our Methocult™ assay.

We also determined changes in myeloid differentiation using the Macrophage-1 antigen (Mac1) and Granulocyte-1 (Gr1) antigen. This analysis identifies myeloid lineage committed cells at various stages of differentiation: $Mac1^{+}Gr1^{-}$ (M1) polymorphonuclear leukocytes/macrophages, $Mac1^{+}Gr1^{+}$ (MG) consists mostly of granulocytes, monocytes and macrophages and $Mac1^{-}Gr1^{+}$ (G1) granulocytes/monocytes. We found a 5-fold increase in the absolute amount of cells double positive for $Mac1^{+}Gr1^{+}$ myeloid precursors, of the macrophage or granulocyte cell lineages (Figure 3D). Our results would suggest that PIAS1 may be required for erythroid differentiation and for repression of granulocyte/macrophage cell lineage differentiation both *in vitro* and *in vivo*.

PIAS1 regulates YS vascular development and gene expression

The YS erythropoiesis and *de novo*-angiogenesis are interrelated processes during embryonic development (Lucitti et al., 2007). To compare the vascular density between *Pias1*$^{+/+}$ and *Pias1*$^{-/-}$ embryos, we performed whole mount IF for PIAS1, *Pecam* (CD31) and smooth muscle actin (SMA-1). Blood vessel size and branching was significantly reduced in *Pias1*$^{-/-}$ embryos (Figure 4A). We selected E12.5 embryos prior to lethality (as assessed by the presence of a beating heart) to determine how *Pias1* deficiency affected expression of genes involved in YS angiogenesis. At this time point the YS is sufficiently developed to allow its dissection and tissue processing. We found that in Pias1$^{-/-}$embryos *Vcam-1* and *Angp2* were significantly reduced compared to *Pias1*$^{+/+}$ controls (* $P<0.05$) (Figure 4B). However, *Vegfr2* was slightly upregulated, suggesting the activation of a compensatory mechanism to promote needed blood vessels. At E12.5, immediately preceding the onset of lethality, heterozygous embryos show a strong induction of *LacZ* in the YS RBC and capillary plexus, while *Pias1*$^{-/-}$ YS have a striking reduction of epithelial thickness, absence of papillary structures and capillaries (Figure 4C, arrows). Thus these findings suggest that, in addition to impaired erythropoiesis, *Pias1* loss may impair angiogenesis in the YS.

Previous work demonstrated that defective erythropoiesis leads to a failure of endothelial cells to form and remodel the YS capillary plexus reduction in erythroblasts will lead to a failure of endothelial cells to form properly remodeling blood vessels in the yolk sac (Lucitti et al., 2007).

To directly address whether *PIAS1* has a cell autonomous role in endothelial cell biology, we performed qPCR analysis of human umbilical vein endothelial cells (HUVECs), following *Pias1* ectopic expression. We analyzed expression of pro-angiogenic and

antiangiogenic genes reported to be responsible for endothelial cell proliferation, survival and migration (Meadows et al., 2013; Dbouk et al., 2014). We found that ectopic expression of *PIAS1* up-regulates *ZEB1, MMP28, WNK1* and *SEMA3A*, a group of genes that promote cell survival and migration. In contrast, ectopic expression of *PIAS1* repressed *THBS1* gene expression; an anti-angiogennic and anti-proliferative gene (Figure 4D). HUVECs are a well-established cellular model used *in vitro* angiogenesis assays based on their ability to form three-dimensional capillary-like tubular structures, when cultured on matrigel. During this assay, HUVECs migrate and polarize into tubular polygonal networks reminiscent of developing capillaries. Notably, we found that *PIAS1 shRNA-mediated* silencing reduced the ability of HUVECs to form branching structures that mimic sprouting blood vessels when grown on matrigel (Figure 4E-F). However, ectopic expression of *PIAS1* alone did not significantly increase HUVEC branching and tube formation *in vitro* (Suppl. Figure 3A-D). We concluded that *PIAS1* is required for the survival of endothelial cells and their ability to form branching structures *in vitro,* but is not sufficient to induce branching.

Pias1 inactivation impairs cardiac development in the mouse embryo

In addition to deterioration of the YS capillary plexus, we noticed that *Pias1*$^{-/-}$ embryos develop cardiomegaly between E9.5 and E12.5. At this stage of embryonic development *Pias1* is expressed predominantly in the neural tube, developing limb buds, gut and heart tissue (Figure 5A). We performed whole mount immunohistochemistry (IHC) for the endothelial marker CD31 in *Pias1*$^{+/+}$ and *Pias1*$^{-/-}$ embryos to detect changes in the embryonic vasculature. Despite the increase in heart size in *Pias1* null embryos, CD31 was significantly reduced in comparison to *Pias1*$^{+/+}$ littermates (Figure 5B; white arrowhead).

To test the relationship between *Pias1* and cardiovascular development we analyzed the gene expression of wild type embryonic hearts with qPCR at several stages of development. We found that CD31, *Vcam-1* and *Pias1* mRNA levels rise and fall together in the developing heart tissue (Figure 5C). Next, we analyzed whether *Pias1* loss affects the heart structural development by performing histological analysis and X-gal staining of heterozygous (*Pias1*$^{+/-}$) and null (*Pias1*$^{-/-}$) embryos at E9.5. At E9.5 we found that there were significantly fewer cells lining the myocardium wall of *Pias1*$^{-/-}$ hearts (Figure 5D). This phenotype worsens overtime as shown by a similar analysis using E11.5 embryos (Figure 5E, black arrows).

Previous reports have suggested a potential role for PIAS1 in cardiac gene regulation (Wang et al., 2004; Wang et al., 2007). To gain insight into how *Pias1* regulates cardiac development, we ectopically expressed *Pias1* in primary myoblasts obtained from E15.5 hearts (Olson et al., 1991; Berkes and Tapscott, 2005; Millay et al., 2013). We selected this specific time point because at E15.5 PIAS1 protein is highly abundant in the liver, the neural tube and heart tissue (Suppl. Figure 4A-B). After establishing short-term myoblast cultures in low serum conditions, we tested for changes in cardiac-specific gene expression following *Pias1* overexpression. We found that *Pias1* expression in primary myoblasts promotes increase of CD31, *MyoD, Myogenin and Myomaker* mRNA, but has no direct effect on *Angp2* or *Vcam-1* genes (Figure 5F). Importantly, these changes in gene expression were

not observed in primary MEFs under the same experimental conditions, suggesting that this is a cardiac specific phenotype (Figure 5G).

Since the progression towards a cardiac-specific developmental program in primary myoblasts is regulated by the expression of cardiac specific transcription factors, we compared *Pias1*, *Myocardin (Myocd)*, *Gata-1* and *Gata-4* gene expression between primary myoblasts and MEFs. Even though we did not find differences in *Pias1* or *Gata-1* expression between primary myoblasts and MEFs, we found significant enrichment for *Myocd* and *Gata-4* mRNAs in primary myoblasts (Suppl. Figure 4C). Moreover, we found that endogenous PIAS1 and GATA-4 protein partially colocalize in myoblasts grown *in vitro* (Suppl. Figure 4D).

These findings suggest that loss of the *Pias1* gene in the mouse embryo impairs cardiac development by affecting the structural development of the myocardium. Moreover, ectopic expression of *Pias1* in primary myoblasts promotes the cardiogenic differentiation program dependent of *Myocd* and/or *Gata-4* gene function.

Pias1 inactivation in endothelial cells is not sufficient to cause embryonic lethality

Our findings indicate that *Pias1* loss results in failure of YS erythropoiesis, capillary plexus development and cardiac muscle defects. These findings prompted us to test whether deleting *Pias1* in endothelial cells would recapitulate the observed phenotypes. To achieve this goal, we crossed $Pias1^{f/f}$ (conditional) mice with a mouse strain that expressed the Cre under the endothelial-specific receptor tyrosine kinase Tie2 ($Tie2^{+/Cre}$) (Koni et al., 2001). Consistent with our previous findings, the YS of $Pias1^{f/f}/Tie2^{+/Cre}$ embryos have significantly fewer erythroid cells when compared to littermate controls (Figure 6A, black arrows). In addition, $Pias1^{f/f}/Tie2^{+/Cre}$ embryos showed reduced blood vessel density in the brain region (head vein) (Figure 6A, white arrow) and occlusion of the connecting stalk (CS), the structure that connects the YS to the embryonic blood vessels (Figure 6 A, green arrow).

Despite these defects, $Pias1^{f/f}/Tie2^{+/Cre}$ embryos showed no growth retardation and the heart and liver size appeared morphologically normal. We performed histological examination of heart and liver tissue to corroborate these findings. Upon close examination of the YS vascularity, we found a significantly reduced capillary plexus in $Pias1^{f/f}/Tie2^{+/Cre}$ embryos when compared to $Pias1^{f/+}/Tie2^{+/Cre}$ littermates (Figure 6B). Moreover, the endothelial cell layer and capillary lumens were significantly reduced contributing to the blockade of RBC circulation in the YS (Figure 6C). The myocardial wall of $Pias1^{f/f}/Tie2^{+/Cre}$ mice had reduced cell density as compared to their wild type littermates (Figure 6D). We found no significant differences in RBC or vascular content between the liver of $Pias1^{f/f}/Tie2^{+/Cre}$ and $Pias1^{+/+}/Tie2^{+/Cre}$ $Pias1^{f/+}/Tie2^{+/Cre}$ littermates (Suppl. Figure 6).

In agreement with the results we obtained in $Pias1^{-/-}$ embryos, we found that $CD71^{+}$ $Ter119^{+}$ double positive cells were reduced in the YS of E9.5 and E11.5 $Pias1^{f/+}Tie2^{+/Cre}$ and $Pias1^{f/f}/Tie2^{+/Cre}$ embryos when compared to $Pias1^{+/+}Tie2^{+/Cre}$ controls (Suppl. Figure 5A). In addition, we observed a twofold increase in $Mac1^{+}Gr1^{+}$ double positive cells in $Pias1^{f/f}Tie2^{+/Cre}$ embryos when compared to $Pias1^{f/+}Tie2^{+/Cre}$ and $Pias1^{+/+}Tie2^{+/Cre}$

littermates at E9.5, which normalized at E11.5 (Suppl. Figure 5B). Despite these defects, we did not observe significant embryonic or perinatal lethality in *Tie2-*$^{Cre/+}$ *Pias1*$^{f/f}$ mice (Suppl. Table 2).

Together our results demonstrate that *Tie2*$^{+/Cre}$ mediated ablation of *Pias1* leads to defective erythropoiesis and endothelial defects in the YS in addition to and modest defects in vasculogenesis and cardiac development in the embryo proper. However, these defects were not sufficient to cause significant embryonic or perinatal lethality.

Discussion

Several studies have investigated the function of *Pias1* in innate immunity, DNA repair and epigenetic regulation (Liu et al., 2004; Galanty et al., 2009; Liu et al., 2014a). However, the role of *Pias1* in embryonic development and tissue differentiation had not been previously studied. In this manuscript we report that *Pias1* loss in mouse embryos results in erythropoietic and angiogenic defects in the YS associated with ~90 % embryonic lethality. The surviving 10% of *Pias1* may be a result of compensation from other Pias family members (*Pias3* or *Pias4*) or members of the SUMOylation machinery such as SUMO E3 ligases or UCB9.

Pias1 loss in early development results in deregulation of embryonic germ layer proliferation, severely decreasing the overall rate of embryonic growth. Consequently, several tissues experience defects in cell proliferation, survival and differentiation. Despite these early gestation defects, our analysis indicates that the most likely cause of embryonic death is the failure to establish and maintain erythropoiesis in the YS during midgestation after E12.5.

Others have shown that between E9.5 and E12.5 erythropoiesis is extremely important to support embryonic growth and survival (Maeda et al., 2009). We found that at this stage of embryonic development, erythroid cells are significantly depleted in the YS of *Pias1* null embryos. Furthermore, we demonstrated that loss of PIAS1 is associated with a block of differentiation at the R2 stage of erythroid differentiation in the YS *in vivo*. Given the crosstalk between endothelial cells and erythroblasts, it is notable that our *in vitro* methylcellulose assays indicate that *Pias1* null erythroid precursors have a cell autonomous defect that prevents their differentiation.

The origin of YS erythroid cell populations, their relationship with the endothelium and contribution to definitive hemopoiesis is still under debate. According to the dominant view endothelial cells are integral part of the hematopoietic stem cell niche and provide support factors to promote the formation of blood islands (Auerbach et al., 1996; Lacaud et al., 2001; Ueno and Weissman, 2006; Myers and Krieg, 2013). Furthermore, it was established that circulating red blood cells actively participate to YS vasculogenesis promoting endothelial remodeling and lumen formation of the developing capillary plexus (Lucitti et al., 2007). Thus, it is possible that the defects in endothelial cell organization are secondary to defective erythropoiesis. Similarly, the observed cardiac defects may be secondary to hypoxia caused by the profound anemia of *Pias1* null embryos or by increased vascular

resistance to blood flow caused by defective vessels and capillaries. To address these possibilities, we performed *in vivo* experiments with $Tie2^{+/cre}$ mice, which ablate *Pias1* in endothelial cells, show that *Pias1* is essential for the formation of the YS capillary plexus and blood islands, but has no obvious effect on liver erythropoiesis and vasculogenesis in the embryo proper. Furthermore, $Tie2^{+/cre}$ mediated inactivation of *Pias1* failed to recapitulate the embryonic lethality caused by constitutive *Pias1* inactivation. Thus, we reason that the defects caused by loss of *Pias1* in the endothelium are not sufficient to cause embryonic lethality. Thus, we conclude that defective fetal erythropoiesis is most likely responsible for the embryonic lethality caused by *Pias1* loss. This conclusion is also supported by the observation that *Pias1* inactivation causes significant hematopoietic cell autonomous defects *in vitro*.

A recent report has described the expansion of tissue resident macrophages originating from YS erythro-myeloid progenitors, independently from definitive hematopoietic stem cells (HSCs) in the liver (Gomez Perdiguero et al., 2015). Constitutive and endothelial cell specific inactivation of *Pias1* gene in developing embryos results in a significant reduction of RBCs and higher number of macrophages in the YS. In light of our findings, we suggest that the EMPs cell compartment within the YS may potentially be regulated by PIAS1 through GATA-1 target genes to induce erythroid differentiation. However, previous reports disagree in whether SUMOylation repress or activates GATA-1 downstream gene transcription (Collavin et al., 2004; Lee et al., 2009; Liu et al., 2014a). In view of our findings, we propose that most likely PIAS1 is a positive regulator of GATA-1 during YS erythropoiesis. Further mechanisms underlying the function of PIAS1 in hematopoietic cells is likely related to the ability of PIAS1 to degrade the PML tumor suppressor, which exerts a well-known pro-apoptotic function (Bernardi and Pandolfi, 2003; Giorgi et al., 2010). Indeed, we found that *Pias1* loss is associated with upregulation of PML and BIM proteins both *in vitro* and *in vivo*.

In addition to YS erythroid deficiency, another finding of our work is that in $Pias1^{-/-}$ embryos, the heart muscle mass is greatly reduced. Histological analysis and X-gal staining confirmed that *Pias1* gene loss results in reduced myocardial wall cellularity and negatively affects cardiac development. *In vitro* assays indicates that *PIAS1* has a cell autonomous involvement in the regulation MYOCD and GATA-4 dependent transactivation of cardiac genes. Previous reports suggest that PIAS1 may play a role in cardiogenic transcription (Wang et al., 2004; Wang et al., 2007; Wang et al., 2008). Thus, our results suggest that PIAS1 may be involved in cardiac muscle development *in vivo*. However, since $Tie2^{+/cre}$ mediated ablation of *Pias1* does not cause significant embryonic lethality, we conclude that *Pias1* is not essential for cardiac development. Instead, it is likely that the lack of proper blood circulation and defective vascular architecture promotes congestive heart failure in $Pias1^{-/-}$ embryos contributing to embryonic lethality after E12.5. Future studies crossing $Pias1^{f/f}$ with Nkx2.5-cre or cTnt-cre mice could more precisely determine the role of *Pias1* in heart muscle development.

Conclusions

Our findings highlight *PIAS1* as an essential regulator of YS erythropoiesis and angiogenesis in the mouse embryo laying the foundation for future studies to determine the role of *Pias1* gene in the hematopoietic system.

Supplementary Material

Refer to Web version on PubMed Central for supplementary material.

Acknowledgements

We thank Lisa Sowels and Margherita Melegari, for administrative assistance and the transgenic technology center at UT Southwestern for ES cell injections. We would also like to thank Dr. Hongtao Yu, Dr. Jerry W. Shay, Dr. Rolf Brekken and Dr. Mariya Ilcheva for helpful discussion and for reviewing this research manuscript. In addition, we like to thank Dr. Ondine Cleaver for constructive comments of the manuscript and sharing the *Tie2*$^{+/Cre}$ mice. This wok was supported by NCI grant #1F31CA180689-01 (to JDC), NIH grants #1R01CA137195, UT Southwestern Friends of the Comprehensive Cancer Center, Texas 4000 (to PPS), #1R01CA172268 (to CCZ) and the Harold C. Simmons Cancer Cennter through NCI Cancer Center support grant 2P30CA016672.

References

1. Auerbach R, Huang H, Lu L. Hematopoietic stem cells in the mouse embryonic yolk sac. Stem cells. 1996; 14:269–280. [PubMed: 8724693]
2. Baudino TA, McKay C, Pendeville-Samain H, Nilsson JA, Maclean KH, White EL, Davis AC, Ihle JN, Cleveland JL. c-Myc is essential for vasculogenesis and angiogenesis during development and tumor progression. Genes & development. 2002; 16:2530–2543. [PubMed: 12368264]
3. Beliakoff J, Lee J, Ueno H, Aiyer A, Weissman IL, Barsh GS, Cardiff RD, Sun Z. The PIAS-like protein Zimp10 is essential for embryonic viability and proper vascular development. Molecular and cellular biology. 2008; 28:282–292. [PubMed: 17967885]
4. Berkes CA, Tapscott SJ. MyoD and the transcriptional control of myogenesis. Seminars in cell & developmental biology. 2005; 16:585–595. [PubMed: 16099183]
5. Bernardi R, Pandolfi PP. Role of PML and the PML-nuclear body in the control of programmed cell death. Oncogene. 2003; 22:9048–9057. [PubMed: 14663483]
6. Coffin JD, Poole TJ. Endothelial cell origin and migration in embryonic heart and cranial blood vessel development. The Anatomical record. 1991; 231:383–395. [PubMed: 1763820]
7. Coffin JD, Harrison J, Schwartz S, Heimark R. Angioblast differentiation and morphogenesis of the vascular endothelium in the mouse embryo. Developmental biology. 1991; 148:51–62. [PubMed: 1936575]
8. Collavin L, Gostissa M, Avolio F, Secco P, Ronchi A, Santoro C, Del Sal G. Modification of the erythroid transcription factor GATA-1 by SUMO-1. Proceedings of the National Academy of Sciences of the United States of America. 2004; 101:8870–8875. [PubMed: 15173587]
9. Conway SJ, Kruzynska-Frejtag A, Kneer PL, Machnicki M, Koushik SV. What cardiovascular defect does my prenatal mouse mutant have, and why? Genesis. 2003; 35:1–21. [PubMed: 12481294]
10. Costa MW, Lee S, Furtado MB, Xin L, Sparrow DB, Martinez CG, Dunwoodie SL, Kurtenbach E, Mohun T, Rosenthal N, et al. Complex SUMO-1 regulation of cardiac transcription factor Nkx2-5. PloS one. 2011; 6:e24812. [PubMed: 21931855]
11. Dbouk HA, Weil LM, Perera GK, Dellinger MT, Pearson G, Brekken RA, Cobb MH. Actions of the protein kinase WNK1 on endothelial cells are differentially mediated by its substrate kinases OSR1 and SPAK. Proceedings of the National Academy of Sciences of the United States of America. 2014; 111:15999–16004. [PubMed: 25362046]

12. Dellinger MT, Meadows SM, Wynne K, Cleaver O, Brekken RA. Vascular endothelial growth factor receptor-2 promotes the development of the lymphatic vasculature. PloS one. 2013; 8:e74686. [PubMed: 24023956]
13. Dunworth WP, Cardona-Costa J, Bozkulak EC, Kim JD, Meadows S, Fischer JC, Wang Y, Cleaver O, Qyang Y, Ober EA, et al. Bone morphogenetic protein 2 signaling negatively modulates lymphatic development in vertebrate embryos. Circulation research. 2014; 114:56–66. [PubMed: 24122719]
14. Feng N, Wang Z, Zhang Z, He X, Wang C, Zhang L. miR-487b promotes human umbilical vein endothelial cell proliferation, migration, invasion and tube formation through regulating THBS1. Neuroscience letters. 2015; 591:1–7. [PubMed: 25660232]
15. Galanty Y, Belotserkovskaya R, Coates J, Polo S, Miller KM, Jackson SP. Mammalian SUMO E3-ligases PIAS1 and PIAS4 promote responses to DNA double-strand breaks. Nature. 2009; 462:935–939. [PubMed: 20016603]
16. Giorgi C, Ito K, Lin HK, Santangelo C, Wieckowski MR, Lebiedzinska M, Bononi A, Bonora M, Duszynski J, Bernardi R, et al. PML regulates apoptosis at endoplasmic reticulum by modulating calcium release. Science (New York, N.Y.). 2010; 330:1247–1251.
17. Gomez Perdiguero E, Klapproth K, Schulz C, Busch K, Azzoni E, Crozet L, Garner H, Trouillet C, de Bruijn MF, Geissmann F, et al. Tissue-resident macrophages originate from yolk-sac-derived erythro-myeloid progenitors. Nature. 2015; 518:547–551. [PubMed: 25470051]
18. Ip HS, Wilson DB, Heikinheimo M, Tang Z, Ting CN, Simon MC, Leiden JM, Parmacek MS. The GATA-4 transcription factor transactivates the cardiac muscle-specific troponin C promoter-enhancer in nonmuscle cells. Molecular and cellular biology. 1994; 14:7517–7526. [PubMed: 7935467]
19. Jacobsen RN, Forristal CE, Raggatt LJ, Nowlan B, Barbier V, Kaur S, van Rooijen N, Winkler IG, Pettit AR, Levesque JP. Mobilization with granulocyte colony-stimulating factor blocks medullar erythropoiesis by depleting F4/80(+)VCAM1(+)CD169(+)ER-HR3(+)Ly6G(+) erythroid island macrophages in the mouse. Experimental hematology. 2014; 42:547–561. e544. [PubMed: 24721610]
20. Kalamarz ME, Paddibhatla I, Nadar C, Govind S. Sumoylation is tumor-suppressive and confers proliferative quiescence to hematopoietic progenitors in Drosophila melanogaster larvae. Biology open. 2012; 1:161–172. [PubMed: 23213407]
21. Kelley C, Blumberg H, Zon LI, Evans T. GATA-4 is a novel transcription factor expressed in endocardium of the developing heart. Development. 1993; 118:817–827. [PubMed: 8076520]
22. Koni PA, Joshi SK, Temann UA, Olson D, Burkly L, Flavell RA. Conditional vascular cell adhesion molecule 1 deletion in mice: impaired lymphocyte migration to bone marrow. The Journal of experimental medicine. 2001; 193:741–754. [PubMed: 11257140]
23. Konstantinov IE, Coles JG, Boscarino C, Takahashi M, Goncalves J, Ritter J, Van Arsdell GS. Gene expression profiles in children undergoing cardiac surgery for right heart obstructive lesions. The Journal of thoracic and cardiovascular surgery. 2004; 127:746–754. [PubMed: 15001903]
24. Lacaud G, Robertson S, Palis J, Kennedy M, Keller G. Regulation of hemangioblast development. Annals of the New York Academy of Sciences. 2001; 938:96–107. discussion 108. [PubMed: 11458531]
25. Lee HY, Johnson KD, Fujiwara T, Boyer ME, Kim SI, Bresnick EH. Controlling hematopoiesis through sumoylation-dependent regulation of a GATA factor. Molecular cell. 2009; 36:984–995. [PubMed: 20064464]
26. Liu B, Yee KM, Tahk S, Mackie R, Hsu C, Shuai K. PIAS1 SUMO ligase regulates the self-renewal and differentiation of hematopoietic stem cells. The EMBO journal. 2014a; 33:101–113. [PubMed: 24357619]
27. Liu B, Mink S, Wong KA, Stein N, Getman C, Dempsey PW, Wu H, Shuai K. PIAS1 selectively inhibits interferon-inducible genes and is important in innate immunity. Nature immunology. 2004; 5:891–898. [PubMed: 15311277]
28. Liu B, Tahk S, Yee KM, Yang R, Yang Y, Mackie R, Hsu C, Chernishof V, O'Brien N, Jin Y, et al. PIAS1 regulates breast tumorigenesis through selective epigenetic gene silencing. PloS one. 2014b; 9:e89464. [PubMed: 24586797]

29. Lucitti JL, Jones EA, Huang C, Chen J, Fraser SE, Dickinson ME. Vascular remodeling of the mouse yolk sac requires hemodynamic force. Development. 2007; 134:3317–3326. [PubMed: 17720695]
30. Maeda T, Ito K, Merghoub T, Poliseno L, Hobbs RM, Wang G, Dong L, Maeda M, Dore LC, Zelent A, et al. LRF is an essential downstream target of GATA1 in erythroid development and regulates BIM-dependent apoptosis. Developmental cell. 2009; 17:527–540. [PubMed: 19853566]
31. McKenna CC, Ojeda AF, Spurlin J 3rd, Kwiatkowski S, Lwigale PY. Sema3A maintains corneal avascularity during development by inhibiting Vegf induced angioblast migration. Developmental biology. 2014; 391:241–250. [PubMed: 24809797]
32. Meadows SM, Ratliff LA, Singh MK, Epstein JA, Cleaver O. Resolution of defective dorsal aortae patterning in Sema3E-deficient mice occurs via angiogenic remodeling. Developmental dynamics : an official publication of the American Association of Anatomists. 2013; 242:580–590. [PubMed: 23444297]
33. Millay DP, O'Rourke JR, Sutherland LB, Bezprozvannaya S, Shelton JM, Bassel-Duby R, Olson EN. Myomaker is a membrane activator of myoblast fusion and muscle formation. Nature. 2013; 499:301–305. [PubMed: 23868259]
34. Myers CT, Krieg PA. BMP-mediated specification of the erythroid lineage suppresses endothelial development in blood island precursors. Blood. 2013; 122:3929–3939. [PubMed: 24100450]
35. Nacerddine K, Lehembre F, Bhaumik M, Artus J, Cohen-Tannoudji M, Babinet C, Pandolfi PP, Dejean A. The SUMO pathway is essential for nuclear integrity and chromosome segregation in mice. Developmental cell. 2005; 9:769–779. [PubMed: 16326389]
36. Olson EN, Brennan TJ, Chakraborty T, Cheng TC, Cserjesi P, Edmondson D, James G, Li L. Molecular control of myogenesis: antagonism between growth and differentiation. Molecular and cellular biochemistry. 1991; 104:7–13. [PubMed: 1922004]
37. Palvimo JJ. PIAS proteins as regulators of small ubiquitin-related modifier (SUMO) modifications and transcription. Biochemical Society transactions. 2007; 35:1405–1408. [PubMed: 18031232]
38. Pang CJ, Lemsaddek W, Alhashem YN, Bondzi C, Redmond LC, Ah-Son N, Dumur CI, Archer KJ, Haar JL, Lloyd JA, et al. Kruppel-like factor 1 (KLF1), KLF2, and Myc control a regulatory network essential for embryonic erythropoiesis. Molecular and cellular biology. 2012; 32:2628–2644. [PubMed: 22566683]
39. Rabellino A, Carter B, Konstantinidou G, Wu SY, Rimessi A, Byers LA, Heymach JV, Girard L, Chiang CM, Teruya-Feldstein J, et al. The SUMO E3-ligase PIAS1 regulates the tumor suppressor PML and its oncogenic counterpart PML-RARA. Cancer research. 2012; 72:2275–2284. [PubMed: 22406621]
40. Rytinki MM, Kaikkonen S, Pehkonen P, Jaaskelainen T, Palvimo JJ. PIAS proteins: pleiotropic interactors associated with SUMO. Cellular and molecular life sciences : CMLS. 2009; 66:3029–3041. [PubMed: 19526197]
41. Shalaby F, Rossant J, Yamaguchi TP, Gertsenstein M, Wu XF, Breitman ML, Schuh AC. Failure of blood-island formation and vasculogenesis in Flk-1-deficient mice. Nature. 1995; 376:62–66. [PubMed: 7596435]
42. Stefater JA 3rd, Lewkowich I, Rao S, Mariggi G, Carpenter AC, Burr AR, Fan J, Ajima R, Molkentin JD, Williams BO, et al. Regulation of angiogenesis by a non-canonical Wnt-Flt1 pathway in myeloid cells. Nature. 2011; 474:511–515. [PubMed: 21623369]
43. Sturgeon CM, Ditadi A, Awong G, Kennedy M, Keller G. Wnt signaling controls the specification of definitive and primitive hematopoiesis from human pluripotent stem cells. Nature biotechnology. 2014; 32:554–561.
44. Sturgeon CM, Chicha L, Ditadi A, Zhou Q, McGrath KE, Palis J, Hammond SM, Wang S, Olson EN, Keller G. Primitive erythropoiesis is regulated by miR-126 via nonhematopoietic Vcam-1+ cells. Developmental cell. 2012; 23:45–57. [PubMed: 22749417]
45. Tamplin OJ, Durand EM, Carr LA, Childs SJ, Hagedorn EJ, Li P, Yzaguirre AD, Speck NA, Zon LI. Hematopoietic stem cell arrival triggers dynamic remodeling of the perivascular niche. Cell. 2015; 160:241–252. [PubMed: 25594182]
46. Tang Y, Harrington A, Yang X, Friesel RE, Liaw L. The contribution of the Tie2+ lineage to primitive and definitive hematopoietic cells. Genesis. 2010; 48:563–567. [PubMed: 20645309]

47. Tsai CT, Ikematsu K, Sakai S, Matsuo A, Nakasono I. Expression of Bcl2l1, Clcf1, IL-28ra and Pias1 in the mouse heart after single and repeated administration of chlorpromazine. Legal medicine. 2011; 13:221–225. [PubMed: 21683644]

48. Ueno H, Weissman IL. Clonal analysis of mouse development reveals a polyclonal origin for yolk sac blood islands. Developmental cell. 2006; 11:519–533. [PubMed: 17011491]

49. Wang J, Feng XH, Schwartz RJ. SUMO-1 modification activated GATA4-dependent cardiogenic gene activity. The Journal of biological chemistry. 2004; 279:49091–49098. [PubMed: 15337742]

50. Wang J, Zhang H, Iyer D, Feng XH, Schwartz RJ. Regulation of cardiac specific nkx2.5 gene activity by small ubiquitin-like modifier. The Journal of biological chemistry. 2008; 283:23235–23243. [PubMed: 18579533]

51. Wang J, Li A, Wang Z, Feng X, Olson EN, Schwartz RJ. Myocardin sumoylation transactivates cardiogenic genes in pluripotent 10T1/2 fibroblasts. Molecular and cellular biology. 2007; 27:622–632. [PubMed: 17101795]

52. Yu L, Ji W, Zhang H, Renda MJ, He Y, Lin S, Cheng EC, Chen H, Krause DS, Min W. SENP1-mediated GATA1 deSUMOylation is critical for definitive erythropoiesis. The Journal of experimental medicine. 2010; 207:1183–1195. [PubMed: 20457756]

Highlights

- *Pias1* loss causes embryonic death between E9.5 and 12.5
- We found that *Pias1* is expressed in rapidly proliferating and in differentiating tissues during development
- *Pias1* ablation leads to embryonic growth retardation and promotes cell death *in vivo* and *in vitro*
- *Pias1* is necessary for erythropoiesis and angiogenesis in the yolk sac
- *Pias1* promotes proper vascular development in the embryo proper
- *Pias1* ablation in endothelial cells recapitulates hematopoietic and angiogenic defects in the yolk sac

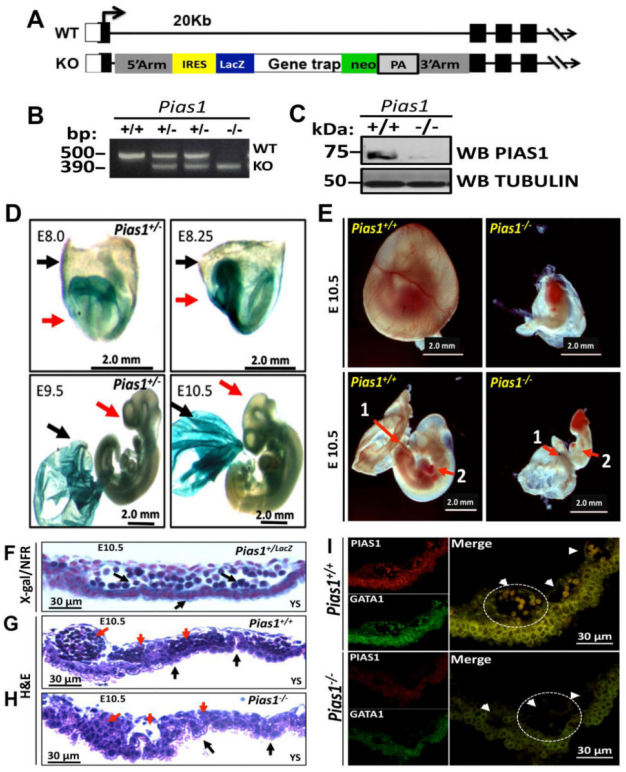

Figure 1. Targeting of *Pias1* leads to severe anemia in the mouse embryo

A, Genomic organization of wild type (WT; *Pias1*$^{+/+}$) and *Pias1* null (KO; *Pias1*$^{-/-}$) alleles generated by gene trap insertion. **B-C,** RT-PCR confirmation of *Pias1* gene disruption and immunoblotting confirmation of PIAS1 protein loss**. D**, Images show the pattern of *Pias1* gene expression determined by X-gal staining at the indicated days of development. Black arrows indicate the YS and red arrows indicate the embryo proper. Scale bar: 2.0 mm. **E**, Comparison of *Pias1*$^{+/+}$ *vs Pias1*$^{-/-}$ embryos at E10.5. Note the significant growth retardation of the *Pias1*$^{-/-}$ embryo. Red arrows indicate areas with reduced blood content in the YS (1) and cardiomegaly (2) in *Pias1* null embryos as compared to their wild type littermates. Scale bar: 2.0 mm. **F,** YS stained with X-gal and nuclear fast red (NFR) at E10.5. Arrows indicate LacZ positivity in capillary beds and RBC within blood islands. **G-H**, Hematoxylin and eosin (H&E) stained YS sections of the indicated genotypes at E10.5. Red arrows indicate RBCs and black arrows supporting vasculature. Note the significant decrease in RBC and abnormal vasculature in the YS of *Pias1*$^{-/-}$. **I,** IF image shows a comparison of YS blood Islands between *Pias1*$^{+/+}$ and *Pias1*$^{-/-}$ embryos at E10.5. Circles indicate positivity for GATA-1 and PIAS1 in blood islands, which are significantly depleted in *Pias1*$^{-/-}$ embryos (arrowheads). Scale bar: 30 µm.

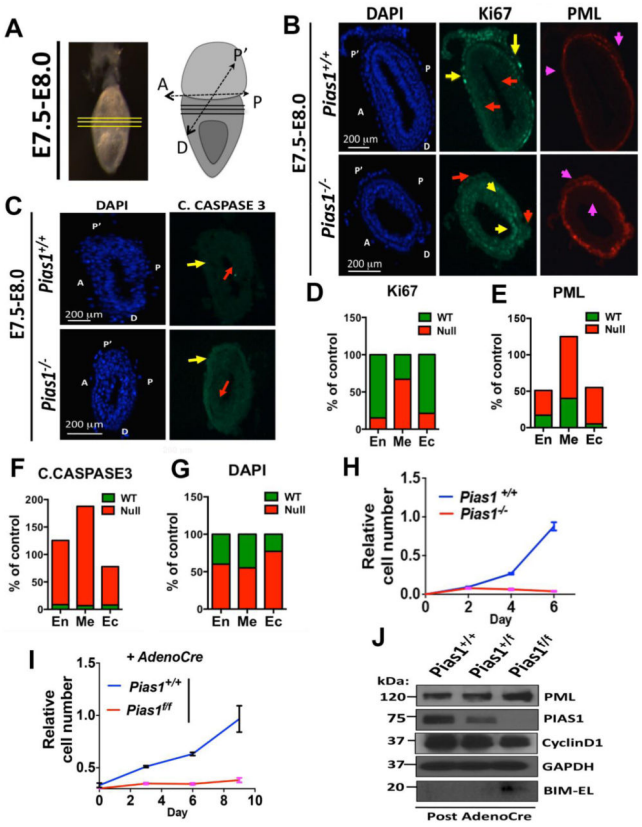

Figure 2. *Pias1* regulates cell proliferation and survival during embryonic development

A, Image of a mouse embryo at E7.5-8.0, the horizontal lines indicate the sites used for transverse sections. The cartoon shows a schematic three-dimensional (3D) rendering of the embryo at this stage of development. Abbreviations; anterior (A), posterior (P), proximal (P') and distal (D) axes. **B**, IF images of *Pias1*$^{+/+}$ and *Pias1*$^{-/-}$ embryonic germ layers stained as indicated. Yellow and red arrows indicate sites of high and low positivity respectively for Ki67 staining in *Pias1*$^{+/+}$ endoderm, mesoderm and ectoderm cells, which appear negative (endoderm) and newly positive (mesoderm-ectoderm) in *Pias1*$^{-/-}$ embryos. Pink arrows indicate PML positivity in mesoderm and endoderm germ layers. Capital letters indicate embryonic axes. **C,** IF images of C.CASPASE-3 positivity in *Pias1*$^{+/+}$ and *Pias1*$^{-/-}$ embryos. Red arrows indicate positivity in mesoderm and ectoderm tissue. Increase positivity for PML is observed in endoderm and mesoderm cells in *Pias1*$^{-/-}$ embryos. **D-G**, Quantification of fluorescence signal intensity from experiments shown in panels B and C; Overlapping green bars indicate *Pias1*$^{+/+}$ and orange bars indicate *Pias1*$^{-/-}$ embryos, respectively. Averaged embryos 3. En: endoderm; Me: mesoderm; Ec: ectoderm. **H**, Proliferation assay of *Pias1*$^{+/+}$ and *Pias1*$^{-/-}$ embryonic cells. Note the reduction in cell proliferation of *Pias1*$^{-/-}$ cells. **I**, Proliferation assay of MEFs of the indicated genotype after exposure to Adeno-Cre. **J**, Immunoblot on MEFs of the indicated genotype after exposure to Adeno-Cre. Note upregulation of the proapoptotic PML and BIM proteins in MEFs after conditional inactivation of *Pias1*. Scale bars: A-B, 200 µm.

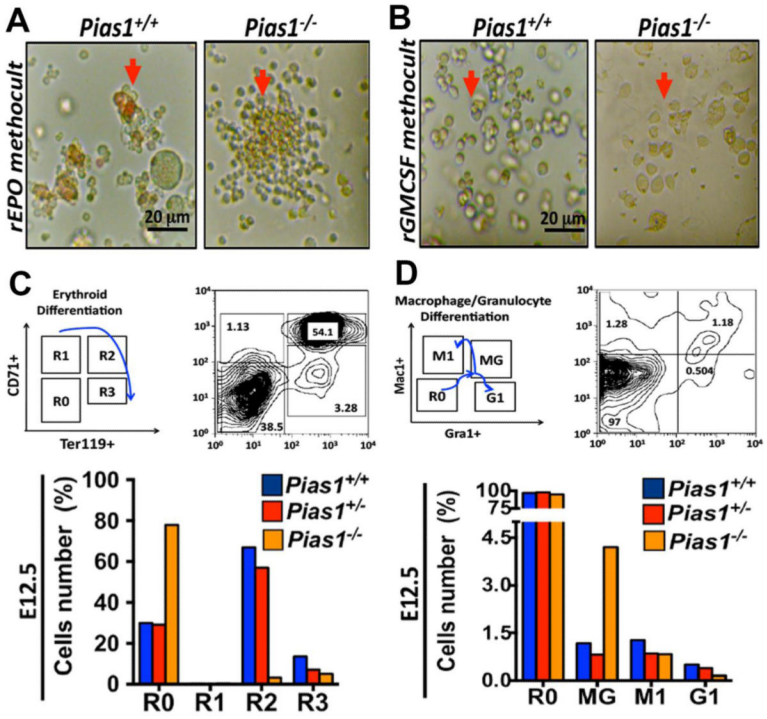

Figure 3. *Pias1* gene loss impairs erythropoiesis in the YS

A, Representative image of a Methocult™ differentiation assay of YS erythroid precursors cells obtained from *Pias1*$^{+/+}$ and *Pias1*$^{-/-}$ embryos using recombinant erythropoietin (rEPO). Note that *Pias1*$^{-/-}$ YS erythroid precursors cells are deficient at forming heme accumulating colonies *in vitro* (red arrows) compared to *Pias1*$^{+/+}$ controls (red arrows). **B**, Representative image of Methocult™ colonies from myeloid precursor cells of the indicated genotype treated with granulocyte and macrophage colony stimulating factor (rGMCSF). Note that *Pias1*$^{-/-}$ colonies show preferential differentiation toward the macrophage cell lineage (red arrows). Scale bar: A-B, 20 µm. **C**, Flow cytometry analysis of *Pias1*$^{+/+}$, *Pias1*$^{+/-}$ and *Pias1*$^{-/-}$ YS cells at E12.5, using CD71^{+} and Ter119^{+} erythroid differentiation markers. Histogram shows reduction in CD71^{+}Ter119^{+} double positive erythroid precursors (R2) and fully differentiated RBCs (R3) in *Pias1*$^{-/-}$ embryos. **D,** Flow cytometry analysis of *Pias1*$^{+/+}$, *Pias1*$^{+/-}$ and *Pias1*$^{-/-}$ YS cells using Mac1^{+} and Gr1^{+} differentiation markers. Histogram shows a fivefold increase in Mac1^{+}Gr1^{+} double positive cells in *Pias1*$^{-/-}$ YS as compared to *Pias1*$^{+/+}$ and *Pias1*$^{+/-}$.

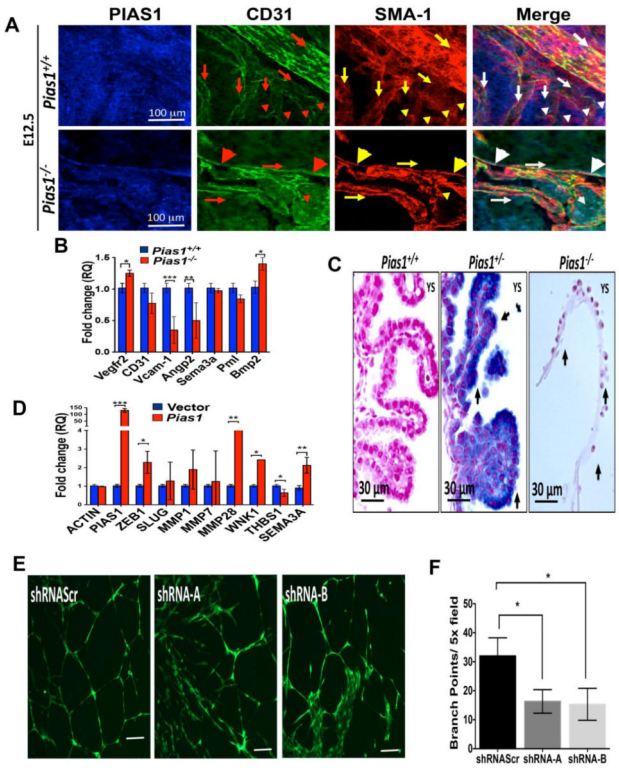

Figure 4. *Pias1* regulates YS angiogenesis and gene expression

A, Whole-mount IF and confocal micrograph of *Pias1*$^{+/+}$ and *Pias1*$^{-/-}$ embryos stained as indicated. Arrows indicate blood vessels, arrowheads capillaries and large arrowheads vessel occlusion. Scale bar: 100 µm. **B,** Histogram shows qPCR expression analysis of the indicated genes in *Pias1*$^{+/+}$ and *Pias1*$^{-/-}$ embryos at the onset of embryonic lethality (E12.5). Note the reduction in *Vcam-1* and *Angp2* gene expression in *Pias1*$^{-/-}$ embryos. n=3 (*: P<0.05). **C**, X-gal staining of the YS capillary plexus of the indicated genotypes. X-gal marks cells expressing *Pias1* in endothelium and RBCs within capillaries at E12.5. **D**, Histogram shows changes in mRNA levels for the indicated genes in HUVECs expressing either empty vector or *Pias1* cDNA. E, Image shows a branch formation assay of HUVECs cells expressing the indicated shRNAs: shRNA Control (shCtrl), shRNA-A and shRNA-B target *PIAS1*. **F**, Histogram shows quantification of branching points per 5x field.

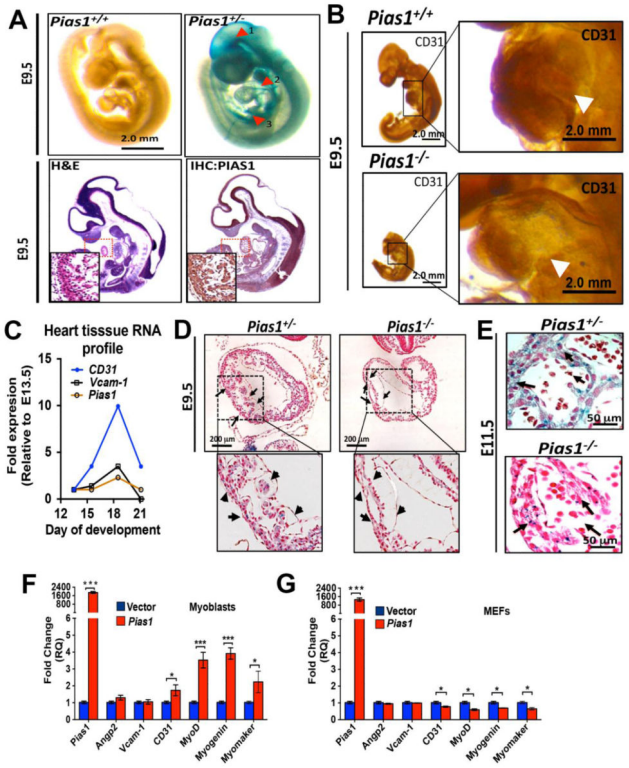

Figure 5. *Pias1* gene loss impairs cardiac development

A, Image shows activation of the *LacZ* reporter inserted into the *Pias1* promoter (upper panels, arrows indicate intense staining of the brain (1), heart (2) and umbilical cord (3) and H&E/IHC (lower panels) for PIAS1 protein in the developing embryo at E9.5. A magnification is provided of the developing heart. **B**, Whole mount IHC stain of the endothelial cell marker CD31 in $Pias1^{+/+}$ and $Pias1^{-/-}$ embryos. Note significantly decreased CD31 staining in $Pias1^{-/-}$ embryonic hearts compared to $Pias1^{+/+}$ littermates (white arrowhead). Scale bar: A-B, 2.0 mm. **C,** qPCR analysis of *CD31*, *Vcam-1* and *Pias1* gene expression at the indicated days of embryonic development. Graph shows a positive correlation between *CD31, Vcam-1* and *Pias1* gene expression in the heart. **D-E,** Histological analysis of embryonic hearts shows reduced cellularity in $Pias1^{-/-}$ embryos (black arrows), and decreased X-gal positive cells compared to $Pias1^{+/-}$ littermates at E9.5. and E11.5. Scale bar: D, 200 µm; E, 50 µm. **F,** qPCR analysis of cardiovascular genes *Angp2*, *Vcam-1*, *Pecam (CD31)*, *MyoD*, *Myogenin* and *Myomaker* in primary myoblasts expressing either empty vector or ectopic *Pias1*. Note significant upregulation of *Pecam*, *MyoD, Myogenin and Myomaker* in primary myoblasts expressing ectopic *Pias1* compared to empty vector.

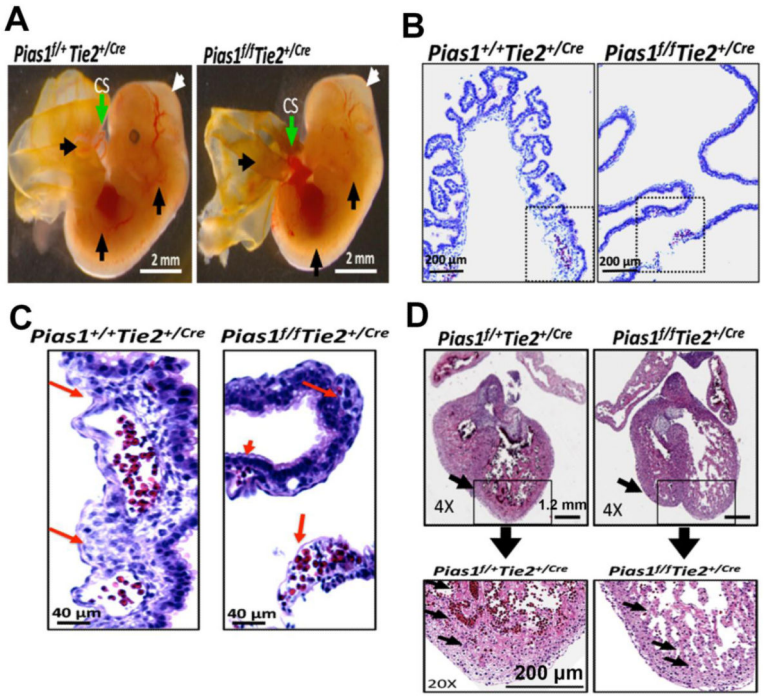

Figure 6. *Pias1* gene deletion in endothelial cells reduces YS erythropoiesis and capillary plexus formation

A, Comparison of *Pias1*$^{f/+}$*/Tie2*$^{+/Cre}$ and *Pias1*$^{f/f}$*/Tie2*$^{+/Cre}$ embryos at E12.5. Black arrows indicate reduced vascularity in the YS and embryo proper. White arrow indicates reduced vascularity into the developing brain region. Green arrow points to the connecting stalk (CS) of the umbilical cord indicating occlusion at YS interface. Scale bars: 2.0 mm. **B and C,** Histological analysis of YS from *Pias1*$^{+/+}$*/ Tie2*$^{+/Cre}$ and *Pias1*$^{f/f}$*/Tie2*$^{+/Cre}$ shows collapsed capillary beds and loss of capillary lumen integrity in *Pias1*$^{f/f}$*/Tie2*$^{+/Cre}$ embryos (red arrows). Scale bar: B, 200 µm; C, 40 µm. **D**, *Pias1*$^{f/+}$*/Tie2*$^{+/Cre}$ and *Pias1*$^{f/f}$*/Tie2*$^{+/Cre}$ embryos heart sections. Scale bar: 1.2 mm. Black arrows indicate sites of high tissue mass and RBC content in *Pias1*$^{f/+}$*/Tie2*$^{+/Cre}$ significantly reduced in *Pias1*$^{f/f}$*/Tie2*$^{+/Cre}$ mice. Scale bar: 1.2 mm and 200 µm.

Table.1

A Percentage (%) of Pias1 animals of all genotypes 4 weeks post birth

Genotype	Gender		Total %
WT 137	Male 76	Female 61	35.0%
Het 212	Male 113	Female 99	55.0%
			9.8%
Null 38	Male 17	Female 21	(*,**)

B. Percentage (%) of Pias1 animals of all genotypes during embryogenesis

Stage	WT	Het	Null	Total
7.5 - 8.5 dpc	9 (25%)	19 (53%)	*8 (22%)	36
9.5 dpc	14 (25%)	32 (56%)	*11 (19%)	57
12.5 dpc	9 (26%)	19 (53%)	**7 (20%)	35
15.5 dpc	11 (25%)	30 (67%)	4 (9%)	45

*Growth retarded embryos

**Dying/dead embryos